33RD CONGRESS
OF THE INTERNATIONAL COUNCIL
OF THE AERONAUTICAL SCIENCES
STOCKHOLM, SWEDEN, 4-9 SEPTEMBER, 2022

ICAS 2022 SWEDEN

PILOT'S ATTENTION DISTRIBUTION MODELING USING HIDDEN MARKOV MODELS

Jiri Hanak[1], Jan Vlk[1] & Peter Chudy[1]

[1]Faculty of Information Technology, Brno University of Technology, tel: +420541141476, fax: +420541141290

Abstract

The attention distribution over an instrument panel serves as a significant indicator of a pilot's cognitive state. Estimation of the attention itself can be performed based on pilot's visual scanning patterns obtained through an eye tracking device. Estimated attention distribution models contribute to the pilot behavior modeling and may also serve the purpose of pilot skill classification. The presented work introduces a pilot study on flight maneuvers classification from pilot gaze fixations, that was investigated on a Light Sport Aircraft flight simulator SimStar, at the Faculty of Information Technology, Brno University of Technology on a focus group of certified pilots.

Keywords: attention distribution, cognition, eye tracking, ground based flight simulator, Hidden Markov Models, maneuver classification, pilot, visual scanning patterns

Nomenclature

a_{ij}	Transition probability from state i to state j
A_{ij}	Absolute count of transitions from state i to state j
$e_i(b)$	Emission probability of output b while Hidden Markov Model is in state i
$E_i(b)$	Absolute count of outputs b while Hidden Markov Model is in state i
M	Number of observed outputs within Hidden Markov Model
N	Number of hidden states within Hidden Markov Model
O	Observed output
s_t	Hidden Markov Model state in time t
α	Forward variable in Forward-Backward algorithm
β	Backward variable in Forward-Backward algorithm
δ	Highest probability for given observed output sequence in Viterbi algorithm
λ	Hidden Markov Model set of parameters
π_i	Probability that hidden state i is the initial state
ψ	Pointer to state which reaches the highest probability in Viterbi algorithm
ξ_t	Transition probability update in Baum-Welch algorithm
AI	Attitude Indicator
ASI	Airspeed Indicator
ALT	Altimeter
DG	Directional Gyro
HMM	Hidden Markov Model
ILS	Instrument Landing System
LSA	Light Sport Aircraft
VSI	Vertical Speed Indicator

1. Introduction

Cognitive pilot models are usually validated through physiological observations such as gaze fixation pattern collections captured by an eye tracking device. The actual gaze tracking is a process of estimating the position of respective gaze fixations in space and mapping them onto elements of the surrounding scene, providing data regarding the participant's fixation locations, screen fixation durations, and the scan path structure in response to a presented stimulus [1]. This information can then be used to study respective task solution strategies and cognitive workload. Therefore, it is not surprising that gaze tracking and its respective parameters have been extensively researched in the military aviation domain in an effort to unobtrusively estimate pilot cognitive workload [2].
Building on the state-of-the-art research, this paper investigates pilot's visual scanning sequences of flight instruments under simulated maneuvering conditions, considering her/his piloting skills and aeronautical knowledge. Common eye movement patterns can be interpreted as similar cognitive strategies in performing a given flight task, moreover, hidden cognitive patterns of respective flight tasks facilitate a plausible model that has a potential to explain the processes and phenomena of Human-Machine Interaction (HMI) [3].

2. Hidden Markov Models

For the purpose of investigating the relation between respective flight maneuvers and associated visual scanning patterns, a Hidden Markov Model (HMM) structure was proposed as the pilot's attention distribution representation. A Markov model is per definition a stochastic model describing randomly changing systems with its current state depending only on the previous state [4]. The state-of-the-art and the most frequent utilization of Markov models is in the area of pattern recognition, i.e. computer science, chemistry, biology, speech or face recognition [5]. The HMMs, as an extended form of Markov models, are composed of two mutually connected groups of states. The hidden states, which are in the presented case the respective flight maneuvers and the observations, which refer to the respective flight instrument the pilot is currently looking at. Hidden states are tied together with a matrix of transition probabilities while the outputs are associated to the hidden states through observation probabilities. Both, transition and observation probabilities are determined from the data acquired during the simulated flight experiment.
As the main use case for the application of the HMM algorithm is the prediction of the pilot's flight maneuver from a sequence of visual scans of the instrument panel, the model structure (hidden states and observations) were carefully selected during the process of pilot modeling to optimally represent a human pilot behavior. The HMM structure and its content can differ with respect to the pilot level of experience or the type of maneuver performed [3]. As stated above, a HMM represents a stochastic model for the description of randomly changing systems. The states of a HMM are, in contrast to Markov chains, by default not directly observable, and are estimated from the observed outputs.
The dependency between the current and previous state can be expressed by the probability of transition from state *i* to state *j* as shown in equation (1).

$$a_{ij} = P(s_t = j | s_{t-1} = i) \tag{1}$$

As mentioned above, the current state of HMM can be determined based on a sequence of observed outputs. From different point of view, the HMM produces observed outputs with a certain probability, which depends on the current hidden state. This probability is known as an emission and it is defined by equation (2), that expresses the probability of observing output *b* if the HMM is currently in the state *i*.

$$e_i(b) = P(O_t = b | s_t = i) \tag{2}$$

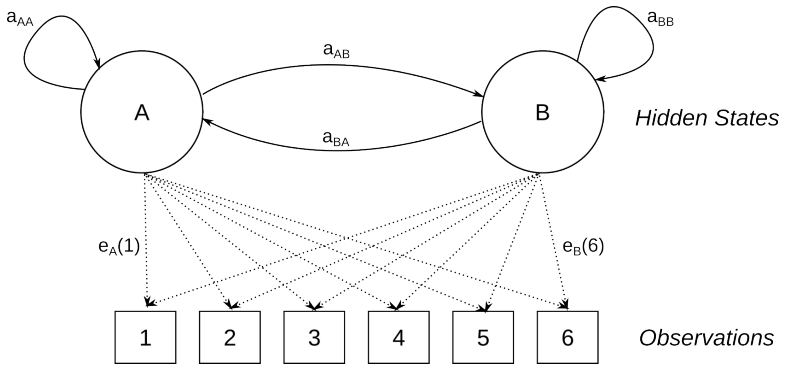

Figure 1 – General structure of a Hidden Markov Model.

Figure 1 shows a general HMM structure with two hidden states and six possible observed outputs. The arrows between states *A* and *B* represent the transition probabilities described by equation (1) and the arrows pointing from states to observed outputs represent the emission probabilities described by equation (2).
The HMM's structure is conveniently described using a matrix formulation, that forms the transition probabilities into a square matrix $N \times N$, where N represents the number of hidden states. Probability that HMM generates specific output while it is in a certain state, i.e. the emission probability is described by matrix $N \times M$, where M represents the number of all possible outputs [6].

2.1 Forward Backward Algorithm

The observed output sequence probability calculation of HMM is solved by employing the Forward-Backward Algorithm, which can be divided into forward and backward parts. For expressing the algorithm's forward part it is necessary to define a forward variable α describing the probability of observed output sequence until the time t and hidden state occurrence in the same time, which can be expressed by equation (3).

$$\alpha_t(i) = P(O_1 O_2 \dots O_t, s_t = i|\lambda) \tag{3}$$

The forward variable calculation is performed iteratively in following steps:

1. Initialization

$$\alpha_1(i) = \pi_i e_i(O_1),\ 1 \leq i \leq N \tag{4}$$

2. Iteration

$$\alpha_{t+1}(j) = \left[\sum_{i=1}^{N} \alpha_t(i) a_{ij}\right] e_j(O_{t+1}),\ 1 \leq t \leq T-1,\ 1 \leq j \leq N \tag{5}$$

3. Termination

$$P(O|\lambda) = \sum_{i=1}^{N} \alpha_T(i) \tag{6}$$

Expressing the sequence of observed outputs is performed by extending the forward algorithm described by equations (4 - 6) by a complete set of observations $O_1, O_2, \dots, O_T$. The same target but reverted approach for probability of observed output sequence calculation is solved by a backward algorithm. Using the backward algorithm involves the definition of backward variable, which expresses the probability that part of the observed output sequence occurs from time $t+1$ to the end of sequence at time T.

$$\beta_t(i) = P(O_{t+1} O_{t+2} \dots O_T, s_t = i|\lambda) \tag{7}$$

The process of the backward variable β calculation is described in a two step iterative approach:

1. Initialization

$$\beta_T(i) = 1,\ 1 \leq i \leq N \tag{8}$$

2. Iteration

$$\beta_t(i) = \sum_{j=1}^{N} a_{ij} e_j(O_{t+1}) \beta_{t+1}(j), t = T-1, T-2, \ldots, 1,\ 1 \leq i \leq N \tag{9}$$

Forward and backward variables are mostly used for the recalculation of HMM parameters within the Baum-Welch algorithm [5].

2.2 Viterbi Algorithm

A method for determination of the most probable hidden state sequence within the HMM is the well known Viterbi algorithm. In other words, it finds the optimal sequence of hidden states, which corresponds to a certain sequence of observed outputs. The approach of Viterbi algorithm can be summarized in following steps:

1. Initialization

$$\delta_1(i) = \pi_i e_i(O_1),\ 1 \leq i \leq N \tag{10}$$

$$\psi_1 = 0 \tag{11}$$

2. Recursion

$$\delta_t(j) = e_i(O_t) \max_{1 \leq i \leq N} \left[\delta_{t-1}(i) a_{ij}\right],\ 2 \leq t \leq T,\ 1 \leq j \leq N \tag{12}$$

$$\psi_t(j) = \operatorname*{argmax}_{1 \leq i \leq N} \left[\delta_{t-1}(i) a_{ij}\right],\ 2 \leq t \leq T,\ 1 \leq j \leq N \tag{13}$$

3. Termination

$$P^* = \max_{1 \leq i \leq N} \delta_T(i) \tag{14}$$

$$s_T^* = \operatorname*{argmax}_{1 \leq i \leq N} \left[\delta_T(i)\right] \tag{15}$$

4. Backward state sequence determination

$$s_t^* = \psi_{t+1}(s_{t+1}^*),\ t = T-1, T-2, \ldots, 1 \tag{16}$$

The variable δ expresses the highest probability for given observed output sequence and defined HMM, while the variable ψ defines a pointer to the state, which reaches the highest probability. The sequence of pointers ψ is used in the terminal phase of the Viterbi algorithm for backward determination of most probable hidden state sequence assuming given sequence of observed outputs [7].

2.3 HMM Parameter Estimation

Two basic situations can occur during the HMM parameter estimation process, i.e. estimation of transition and emission probability matrices. In the first case the training dataset contains a sequence of observed outputs as well as respective sequence of hidden states. In this case the HMM parameter estimation is performed by expressing the relative counts of transitions between states and observed outputs. Equations (17 - 18) define the estimates of transition and emission probabilities resulting from maximum likelihood algorithm [8].

$$a_{ij} = \frac{A_{ij}}{\sum_{j'} A_{ij}} \tag{17}$$

$$e_i(b) = \frac{E_i(b)}{\sum_{b'} E_i(b')} \tag{18}$$

The probability of transition from the state i to state j expressed by the equation 17 is defined as a ratio between the number of transitions from the state i to the state j and the number of all transitions from the state i in the training dataset. Probability of emitting an observed output b while the HMM remains in the state i expressed by equation 18 is defined as a ratio between the number of observed output b emissions from the state i and the number of all observed emissions from the state i.
When the training dataset contains only the sequence of observed outputs, the parameter estimation is not performed directly, instead a re-estimation of a'priori probabilities is executed, which employs the iterative Baum-Welch algorithm [8]. This method estimates the new transition and emission probabilities based on observed output sequences and calculations performed by Forward-Backward algorithm described in the previous subsection. The first step is expressing the transition probability from the state i to the state j for specific sequence of observed outputs and a'priori given HMM parameters, which can be described by equation (19).

$$\xi_t(i,j) = P(s_t = i, s_{t+1} = j | O, \lambda) \tag{19}$$

Utilizing the forward and backward variables allows us to redefine the equation (19) to following expression.

$$\xi_t(i,j) = \frac{\alpha_t(i) a_{ij} e_j(O_{t+1}) \beta_{t+1}(j)}{\sum_{i=1}^{N} \sum_{j=1}^{N} \alpha_t(i) a_{ij} e_j(O_{t+1}) \beta_{t+1}(j)} \tag{20}$$

The equation (20) enables to express the probability that the HMM is in a hidden state i at time t and transits to a state j in time $t+1$ assuming certain observed output sequence and a'priori knowledge of the HMM parameters.

$$\gamma_t(i) = \sum_{j=1}^{N} \xi_t(i,j) \tag{21}$$

The re-estimation of HMM parameters, by employing equations (20-21), is expressed in equation (22) that describes the probability of transition between states and equation (23), which defines the probability of emitting certain observed output while the HMM is in a specific state [9].

$$\bar{a}_{ij} = \frac{\sum_{t=1}^{T-1} \xi_t(i,j)}{\sum_{t=1}^{T-1} \gamma_t(i)} \tag{22}$$

$$\bar{e}_j(b) = \frac{\sum_{\substack{t=1 \\ O_t = b}}^{T-1} \gamma_t(j)}{\sum_{t=1}^{T-1} \gamma_t(j)} \tag{23}$$

3. Maneuver Classification Using HMM

A convenient utilization of the HMM in pilot behavior modeling is the classification of flight maneuvers based on visual attention distribution over the aircraft's instrument panel, i.e. scanning patterns. The identification of a flight maneuver is performed using measured gaze fixations in the pilot's work space. The measurement itself is executed using a device for the eye movement tracking, the gaze tracker. The HMM-based pilot model contains following hidden states and observed outputs:

- Hidden states — representation of a specific flight maneuver (steady level flight; climb or descent; level, climbing or descending turn; ILS approach).
- Observed output — representation of a specific flight instrument, at which the pilot is fixing her/his attention (Airspeed Indicator, Attitude Indicator, Altimeter, Directional Gyro, Vertical Speed Indicator, ILS instrument, Timer).

The estimation of HMM parameters is performed using a set of measured data containing gaze fixation sequences in respective flight maneuvers. Figure 2 illustrates a HMM structure with seven hidden states and seven possible observation outputs for the pilot attention distribution model.

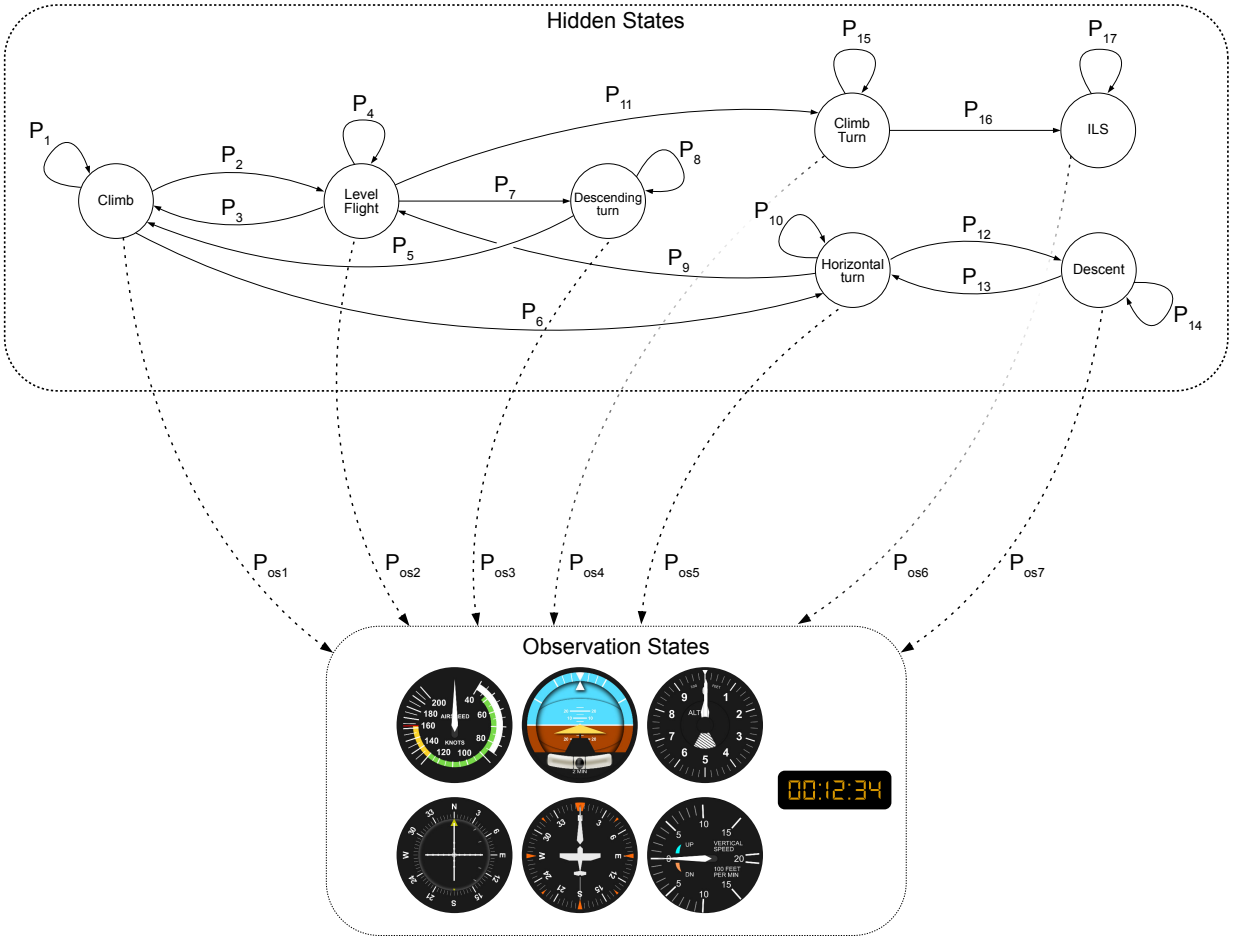

Figure 2 – Pilot's behavior modeled using HMM.

4. Simulator Flight Experiment

The simulated flight experiment has been performed on a fixed base Light Sport Aircraft (LSA) simulator SimStar equipped with an analog instrument panel containing an Airspeed Indicator (ASI), Attitude Indicator (AI), Altimeter (ALT), Instrument Landing System (ILS) indicator, Directional Gyro (DG), Vertical Speed Indicator (VSI) and a Timer. Figure 3 shows the SimStar's simulation environment utilized in the simulated flight experiments.

(a) Simulator cockpit. (b) Instrument panel.

Figure 3 – Simulation environment.

A focus group of qualified pilots has been instructed to perform series of simulated flights composed of flight maneuvers described in Table 1 and defined by respective target Airspeed, Altitude and Heading quantities. These pilots have been instructed to perform turns with a limited turn rate of $3°{\cdot}s^{-1}$, while all climb and descent maneuvers had their vertical speed limit set to 500 $ft{\cdot}min^{-1}$ and -500 $ft{\cdot}min^{-1}$, respectively. The level flights with ID numbers #3 and #9 were pre-planned to take two and one minute of flight time, respectively. Pilots were also instructed to deploy flaps to 15° during the phase #11 before the LOC capture.

Table 1 – Flight maneuvers specification.

ID	Maneuver	IAS [kts]	ALT [ft]	HDG [°]
#1	Take-Off	75	800 → 1000	93
#2	Climb	75	1000 → 3000	90
#3	Level flight	100	3000	90
#4	Descending turn	90	3000 → 2500	90 → 270
#5	Climb	75	2500 → 3000	270
#6	Horizontal turn	100	3000	270 → 90
#7	Descent	100 → 90	3000 → 2500	90
#8	Horizontal turn	90	2500	90 → 135
#9	Level flight	100	2500	135
#10	Climb turn	90	2500 → 3000	135 → 315
#11	LOC capture	90 → 75	3000	315 → 273
#12	GS capture	75	3000	273
#13	ILS approach	75	3000 → 1080	273
#14	Decision altitude	75	1080	273

Flight maneuvers described in Table 1 are shown in the reference trajectory introduced in Figure 4. The reference trajectory contains color-coded sequences of respective flight maneuvers with an associated legend to emphasize a clear understanding of the trajectory. The blue segments indicate change in Altitude, while the green segments represent horizontal maneuvering. The initial and final parts of the trajectory, i.e landing and touchdown, are marked in red color.

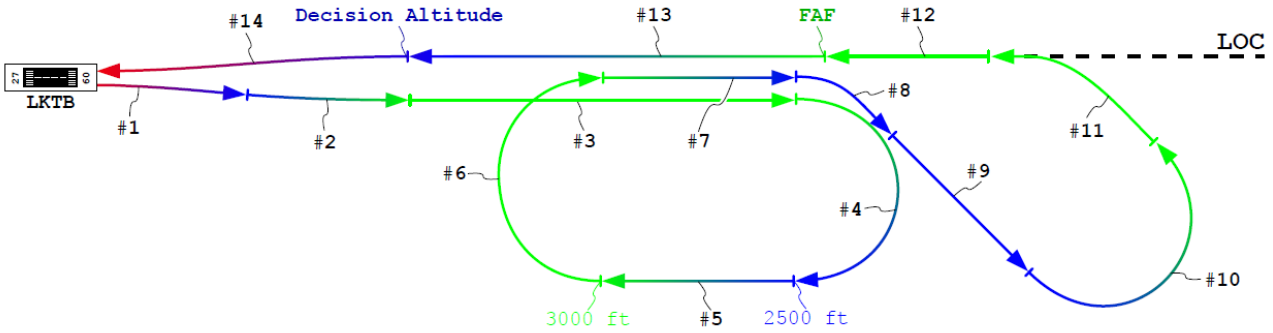

Figure 4 – Reference trajectory with marked flight phases.

Pilots taking part in the experiment were asked to wear a gaze tracking headset composed of two eye cameras and one world camera, which recorded their gaze fixations over the instrument panel during the simulated flight in SimStar flight simulator. The video recording frequency was set to 60 Hz and the resolution to 720p. Figure 5 shows the gaze tracking device used for gaze fixation recordings.

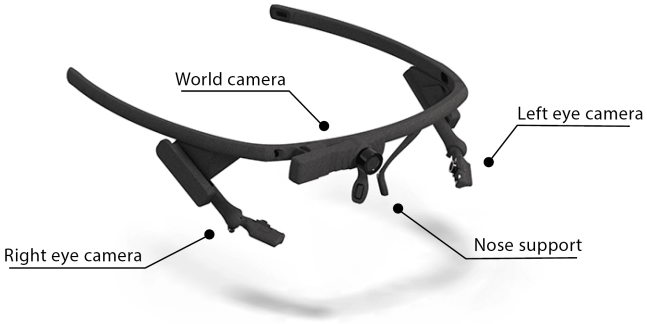

Figure 5 – Gaze tracking device [10].

Another type of data recorded during the flight experiment on the SimStar were flight variables associated to basic aircraft kinematics: translational and rotational accelerations and velocities, aircraft attitude and position. These kinematic data were recorded at a sampling rate of 30 Hz and used in flight maneuver labeling, which is an inevitable asset in the HMM training phase. Figure 6 shows a recorded trajectory of the experimental flight near Brno's LKTB airport in Czechia, Europe.

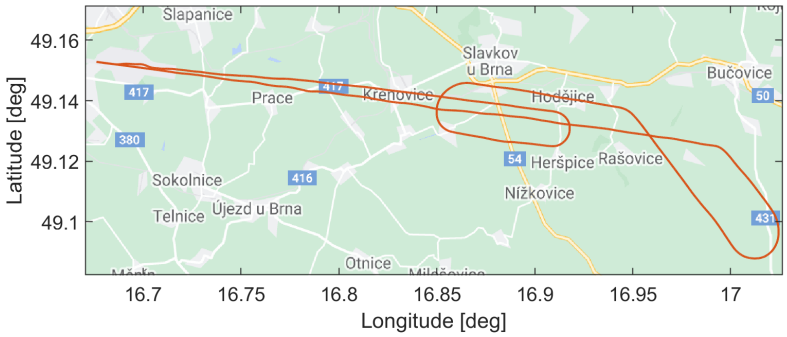

Figure 6 – Flight experiment trajectory.

5. Results

As the main task of the pilot's attention distribution model is the flight maneuver classification based on gaze fixation sequences over an instrument panel, the measured data had to be pre-processed and labeled to match the simulated flight trajectory description introduced in the previous section. The maneuvers to be determined by the HMM were the climb, steady level flight, descent, climbing turn, horizontal turn, descending turn and an ILS approach. The take-off and landing phases were not considered in the HMM design as they mostly contain gaze fixations "outside of the aircraft" which add a high uncertainty into the attention distribution model. Figure 7 shows the main flight quantities, Airspeed, Altitude and Heading, segmented using differently colored labels for respective flight maneuvers. The HMM's hidden states are in our case represented by the flight maneuver labels, thus the time series of flight maneuver labels were used as the output in the HMM parameter estimation. The input data used for pilot's attention distribution model training were the gaze fixations over the SimStar's instrument panel.

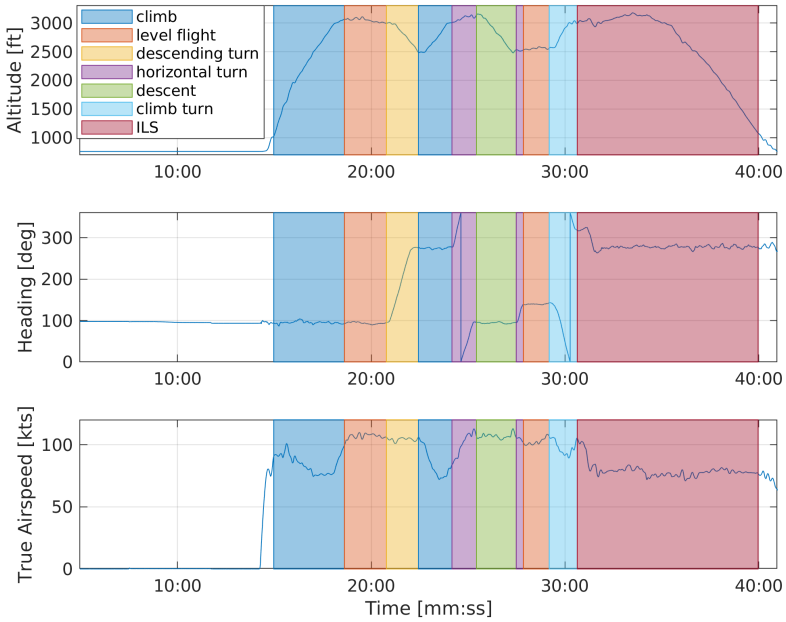

Figure 7 – Flight segmented into maneuvers.

The gaze fixation time threshold was set to 200 ms, while shorter fixations were considered saccade points, i.e. rapid eye movement, and were not considered. Fixations longer than 500 ms were divided into multiple subsequent fixations to match the purpose of model training. In order to assign each fixation to a specific instrument on the instrument panel, the K-means clustering / segmentation algorithm was employed [11]. In the presented case, fixations were mapped into 7 clusters corresponding to SimStar's flight instruments mentioned in the previous section. Figure 8 shows the gaze fixations segmented into respective colored clusters. In other words, valid fixation points get their labels based on the respective "looked at" instrument (ASI, AI, ALT, etc.). Time series of instrument labels represent the observed HMM outputs.

The dataset for pilot's attention distribution model training is a combination of the data recorded in six simulated flights performed by a focus group of two qualified pilots, both of which were male participants with an average age of 21 years, average flight time of 240 hours and total flight time in last 30 days averaging at 9 hours. One participant had experience in instrument flying while the other one did not.

The time sequence of gaze fixations represents observed outputs and corresponding sequence of flight maneuver labels is considered to represent hidden states. The results of the training process, described by equations (17-23) in Section 2.3, are the estimated HMM parameters representing the pilot's attention distribution model, i.e. the HMM transition and emission matrices.

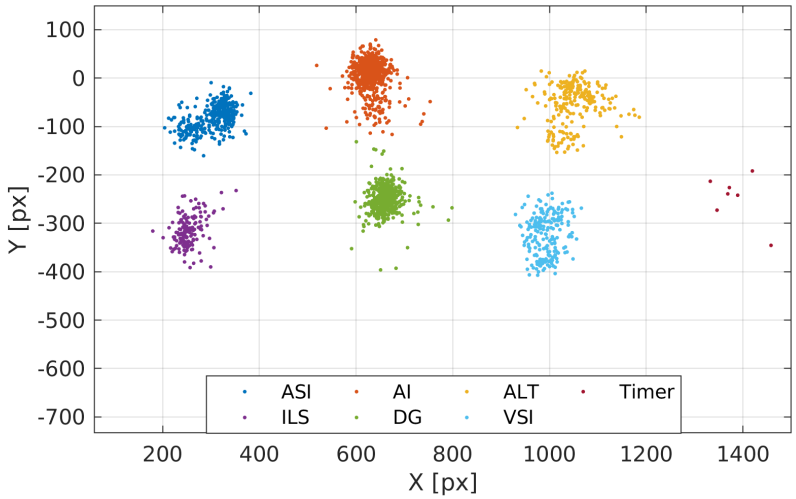

Figure 8 – Pilot's clustered gaze fixations.

The trained HMM was evaluated using labeled data, i.e. fixations and flight maneuvers, from another flight. Figure 9 shows an example of fixation label time series (first graph) and flight maneuver labels (second graph). Signal in the first graph shows the pilot switching gaze fixations between instruments in time. The second graph contains time series of ground truth flight maneuver labels (blue) as well as the HMM outputs generated by the Viterbi algorithm (red). The trained model was able to successfully determine 92 % of flight phases based on measured gaze fixations.

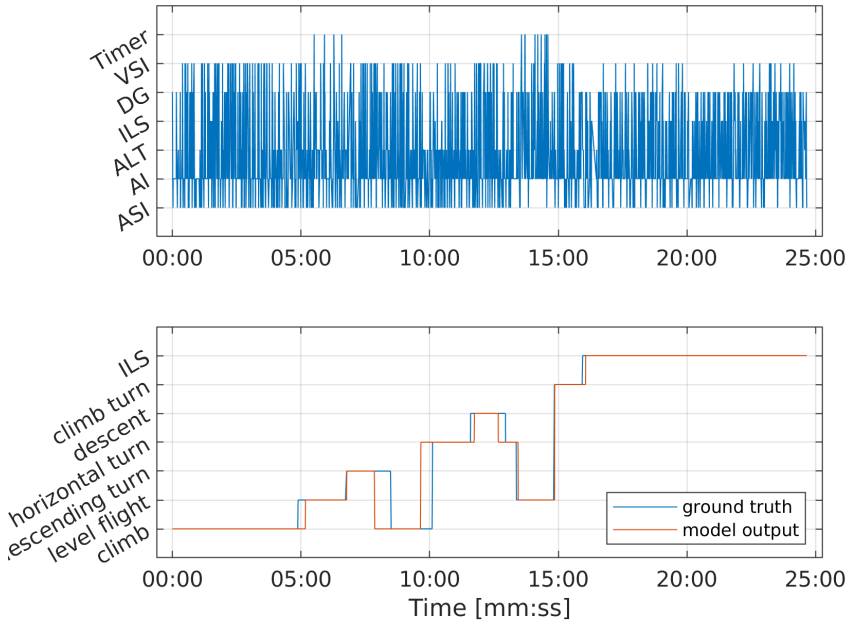

Figure 9 – Pilot HMM evaluation.

Figure 10 shows a relative ratio of gaze fixations over different instruments with respect to the specific flight maneuver. Graphs are based on the training dataset and in fact represent a graphical interpretation of the HMM's emission matrix. The attention distribution in Figure 10 shows, for example, that the most used instrument during the whole flight is the AI, with a quite similar attention distribution through all investigated flight maneuvers. However, some differences can be observed, e.g. higher

fixation counts at VSI during the descent or utilization of an ILS instrument in the final approach phase of the flight.

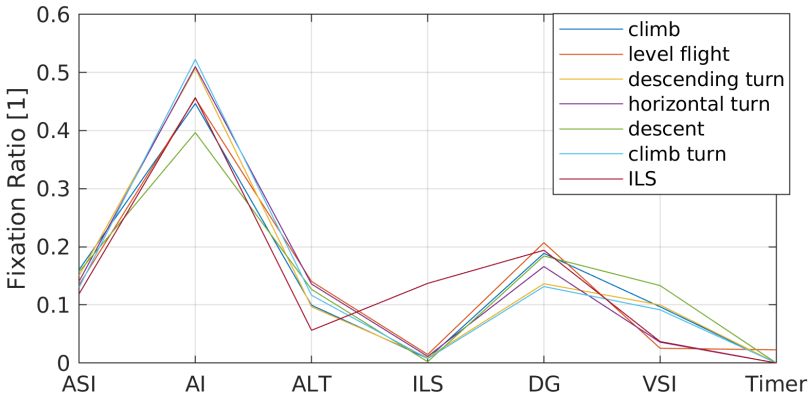

Figure 10 – Attention distribution over instrument panel.

6. Conclusion

This paper introduces an HMM representation of pilot's attention distribution over an aircraft instrument panel with respect to a specific flight maneuver. It discusses an experimental study on flight maneuver classification from pilot's gaze fixations. The data for the HMM model training were collected in series of simulated flight experiments performed on a realistic LSA simulator, SimStar, at the Faculty of Information Technology, Brno University of Technology, with a focus group of qualified pilots. Results presented in Section 5 show the capability of the trained HMM to classify current flight maneuver based on pilot's measured gaze fixations. Findings obtained through the HMM models will further help to refine cognitive pilot model designs using modern cognitive architectures. Such models could be useful in the process of future cockpit design or as an objective measure during a pilot training evaluation.

Acknowledgments

This project is co-financed from the state budget by the Technology agency of the Czech Republic under the National Centres of Competence 1 Programme: Support programme for applied research, experimental development and innovation. Subproject TN01000029/16 Tactical Cognitive Agent.

Copyright Statement

References

[1] D. B. Mohan, G. Prabhakar, P. Biswas, and J. Shree. Using eye gaze tracker to automatically estimate pilots' cognitive load. 06 2019.

[2] J. Tole, A. Stephens, Michel Vivaudou, Arye Ephrath, and L Young. Visual scanning behavior and pilot workload. *NASA Contractor Reports*, 09 1983.

[3] M. Hayashi. *Hidden Markov Models for Analysis of Pilot Instrument Scanning and Attention Switching*. PhD thesis, Massachusetts Institute of Technology, 9 2004.

[4] L. Rabiner and B. Juang. An introduction to hidden markov models. *IEEE ASSP Magazine*, 3(1):4–16, 1986.

[5] R. Durbin, S. R. Eddy, A. Krogh, and G. Mitchison. *Biological Sequence Analysis: Probabilistic Models of Proteins and Nucleic Acids*. Cambridge University Press, 1998.

[6] L.R. Rabiner. A tutorial on hidden markov models and selected applications in speech recognition. *Proceedings of the IEEE*, 77(2):257–286, 1989.

[7] A. Viterbi. Error bounds for convolutional codes and an asymptotically optimum decoding algorithm. *IEEE Transactions on Information Theory*, 13(2):260–269, 1967.

[8] Y. Boussemart, M.L. Cummings, J. Las Fargeas, and N. Roy. Supervised vs. unsupervised learning for operator state modeling in unmanned vehicle settings. *Journal of Aerospace Computing, Information, and Communication*, 8(3):71–85, 2011.

[9] G. Khodabandelou, C. Hug, R. Deneckere, and C. Salinesi. Supervised vs. unsupervised learning for intentional process model discovery. *Business Process Modeling, Development, and Support*, pages 1–15, 2014.

[10] PSYCHOPY.ORG. Pupil labs - core. `https://psychopy.org/api/iohub/device/eyetracker_interface/PupilLabs_Core_Implementation_Notes.html`. Accessed: 2022-05-30.

[11] C. M. Bishop. *Neural Networks for Pattern Recognition*. Oxford University Press, Inc., USA, 1995.